工學碩士 學位論文

Characteristics of Al-doped ZnO film grown by DC magnetron sputtering for an application of solar cell

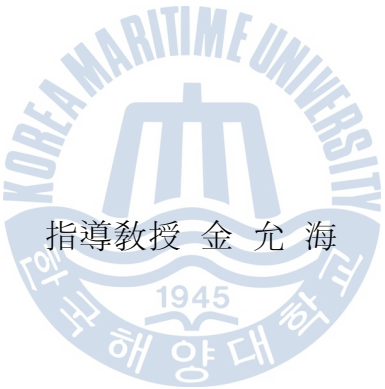

指導敎授 金 允 海

2014년 7월

韓國海洋大學校 大學院

材 料 工 學 科

朴 昶 昱

本 論文을 朴昶昱의 工學碩士 學位論文으로 認准함.

위원장　　文 慶 萬　　(인)

위　원　　河 鎭 喆　　(인)

위　원　　金 允 海　　(인)

2014년 7월

韓國海洋大學校 大學院

Contents

List of Tables

List of Figures

Characteristics of Al-doped ZnO film grown by DC magnetron sputtering for an application of solar cell

Park, Chang Wook

Department of Materials Engineering

Graduate School of Korea Maritime and Ocean University

Abstract

Transparent Conductive Oxides (TCO) is a thin film to be used in numerous applications throughout the industry in general. Representative Industry have been used for the electrodes used in the touch panel and the LCD to be used for transparent electrodes in flat display industry of the display industry. Application of the substrate and the electrode of the solar cell have been many studies now. Transparent electrode materials used in these industries are in need of light transmittance higher low electrical characteristics are excellent, substances showing the most excellent physical properties while satisfying all the characteristics such (Indium Tin Oxide) 's film. However, indium, high reserves is small, there is an environmental pollution problem. So study of ZnO is actively carried out in an alternative material. This study analyzed the characteristics by using a DC magnetron sputtering system. The electric and

optical properties of these films were studied by Hall measurement and optical spectroscopy, respectively. When the Al target input current are 2mA and 4mA, it demonstrate about 80% transmittance in the range of the visible spectrum. Also, When Al target input current was 6mA, sheet resistance is the smallest on glass and PET substrate. The minimum resistivity are 4.51×10^{-3}ohm/sq. and 3.96×10^{-3}ohm/sq.

KEY WORDS: Transparent conductive oxide, Al doped ZnO, Electrical property, DC magnetron sputtering, Hall measurements, Organic solar cell, Optical property,

1. Introduction

TCO(transparent conducting oxide) is high electrical conductivity properties and optical transmittance at a wavelength of 400 ~ 800nm is an excellent films. TCO is started by Badeker at 1907 years Cd oxide film fabricated by sputtering method, nowadays, with the development of science and industry is required to have high-quality TCO. At present, thins films are generally needed as transparent electrodes in practical applications, because of their low resistivity, on the order of 10^{-4} Ω•cm, and stable electrical, optical and mechanical properties. Oxide films including Indium Tin Oxide (ITO), Indium Zinc Oxide (IZO), Aluminum Zinc Oxide (AZO), and ZnO are representative among many types of the transparent electrodes; particularly, ITO possesses excellent physical and chemical stability such as adhesiveness and rigidity for various types of boards as well as transmittance and electric conductivity there by utilizing in many fields[4]. [H. Czternastek, Opto-Electronics Review 12, 49 (2004)] However, ITO is a relatively expensive material because indium is not abundant. On the other hand, ZnO could be useful as a less expensive coating material than ITO if a thin film deposition technique can extract highly conductivity and high physical properties from ZnO at low cost. Al-doped ZnO (AZO) is a particularly attractive material because of its

excellent properties, such as higher thermal stability, lower resistance against damage by hydrogen plasma and lower cost of fabrication, compared to ITO. [25] [C.G. Granqvist, Thin Solid Films (1990) 730, pp.193-194] Various methods, such as sputtering, Pulse Laser Deposition (PLD), Evaporation, Spray pyrolysis, Sol-gel preparation and Electrochemical deposition, are used to fabricate AZO thin films. Sputtering is a thin film of uniform particles can be coated with a homogeneous. So suitable for the manufacture of ultra thin film. And sputtering method is possible deposited at a low temperature because been widely used in the manufacture of TCO. Also, solar energy has advantages of non environmental pollution, zero noise making, and a source of infinite energy creation unlikely fossil energy. More than 90% of the solar industry is si-based. The advantages of organic solar cell is manufacturing process is very simple, the price is cheap, can make flexible cell. However, the power conversion efficiency by around 5%, it will take more time to commercialization.

In this report, applications of the organic solar cell to the transparent electrode AZO thin film produced by dc magnetron sputtering and evaluated. We describe the effects of the aluminium concentration on zinc oxide thin films, which have a great impact on the optical and electrical properties of AZO thin films.

2. Background

2.1 ZnO

ZnO is a wide-bandgap semiconductor of the II-VI semiconductor group (since oxygen was classed as an element of VIA group (the 6th main group, now referred to as 16th) of the periodic table and zinc, a transition metal, as a member of the IIB (2nd B), now 12th, group). The native doping of the semiconductor (due to oxygen vacancies or zinc interstitials)[4] is n-type. This semiconductor has several favorable properties, including good transparency, high electron mobility, wide bandgap, and strong room-temperature luminescence. Those properties are used in emerging applications for transparent electrodes in liquid crystal displays, in energy-saving or heat-protecting windows, and in electronics as thin-film transistors and light-emitting diodes.

2.1.1 Structure

Zinc oxide crystallizes in two main forms, hexagonal wurtzite and cubic zinc blende. The wurtzite structure is most stable at ambient conditions and thus most common. The zinc blende form can be stabilized by growing ZnO on substrates with cubic lattice structure. In

both cases, the zinc and oxide centers are tetrahedral, the most characteristic geometry for Zn(II). ZnO converts to the rocksalt motif at relatively high pressures about 10 GPa.

Hexagonal and zinc blende polymorphs have no inversion symmetry (reflection of a crystal relative to any given point does not transform it into itself). This and other lattice symmetry properties result in piezoelectricity of the hexagonal and zinc blende ZnO, and pyroelectricity of hexagonal ZnO. The hexagonal structure has a point group 6 mm (Hermann-Mauguin notation) or C_{6v} (Schoenflies notation), and the space group is $P6_3mc$ or C_{6v}^4. The lattice constants are a = 3.25 Å and c = 5.2 Å; their ratio c/a ~ 1.60 is close to the ideal value for hexagonal cell c/a = 1.633. As in most group II-VI materials, the bonding in ZnO is largely ionic (Zn^{2+}–O^{2}–) with the corresponding radii of 0.074 nm for Zn^{2+} and 0.140 nm for O^{2-}. This property accounts for the preferential formation of wurtzite rather than zinc blende structure, as well as the strong piezoelectricity of ZnO. Because of the polar Zn-O bonds, zinc and oxygen planes are electrically charged. To maintain electrical neutrality, those planes reconstruct at atomic level in most relative materials, but not in ZnO – its surfaces are atomically flat, stable and exhibit no reconstruction. This anomaly of ZnO is not fully explained yet.

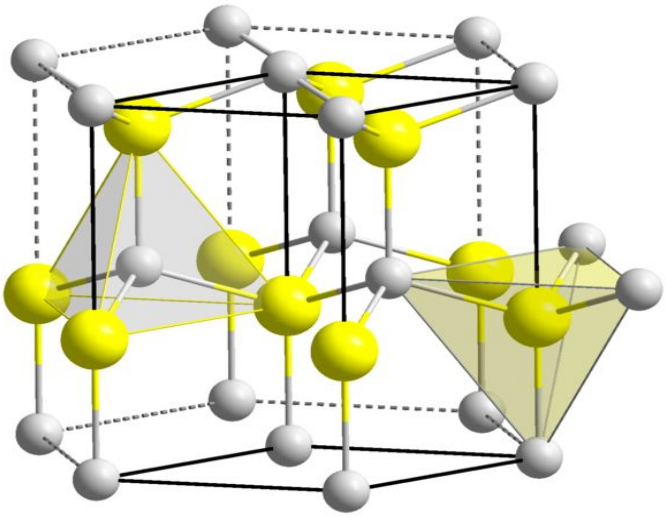

Fig. 1 Wurtzite structure

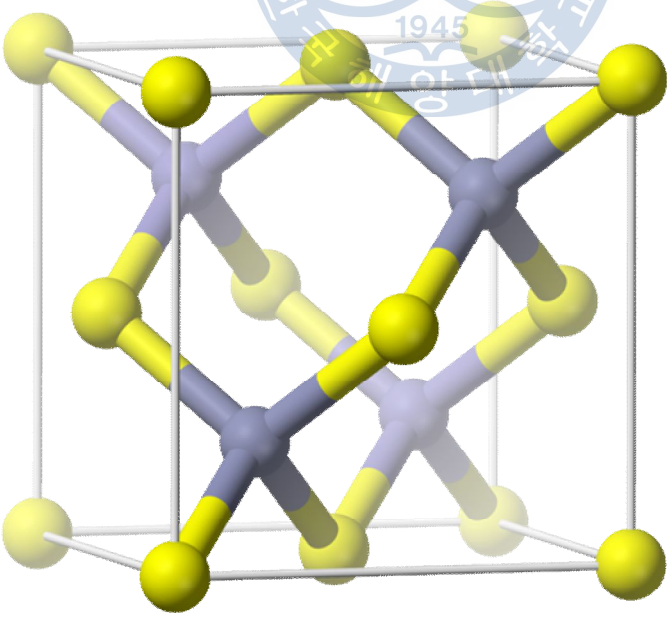

Fig. 2 A zinc blende unit cell

2.1.2 Mechanical properties

ZnO is a relatively soft material with approximate hardness of 4.5 on the Mohs scale. Its elastic constants are smaller than those of relevant III-V semiconductors, such as GaN. The high heat capacity and heat conductivity, low thermal expansion and high melting temperature of ZnO are beneficial for ceramics. ZnO exhibits a very long lived optical phonon E2(low) with a lifetime as high as 133 ps at 10 K. Among the tetrahedrally bonded semiconductors, it has been stated that ZnO has the highest piezoelectric tensor, or at least one comparable to that of GaN and AlN. This property makes it a technologically important material for many piezoelectrical applications, which require a large electromechanical coupling.

2.1.3 Electrical properties

ZnO has a relatively large direct band gap of ~3.3 eV at room temperature. Advantages associated with a large band gap include higher breakdown voltages, ability to sustain large electric fields, lower electronic noise, and high-temperature and high-power operation. The bandgap of ZnO can further be tuned to ~3–4 eV by its alloying with magnesium oxide or cadmium oxide.

Most ZnO has n-type character, even in the absence of intentional doping. Nonstoichiometry is typically the origin of n-type character, but the subject remains controversial. An alternative explanation has been proposed, based on theoretical calculations, that unintentional substitutional hydrogen impurities are responsible. Controllable n-type doping is easily achieved by substituting Zn with group-III elements such as Al, Ga, In or by substituting oxygen with group-VII elements chlorine or iodine. Reliable p-type doping of ZnO remains difficult. This problem originates from low solubility of p-type dopants and their compensation by abundant n-type impurities. This problem is observed with GaN and ZnSe. Measurement of p-type in "intrinsically" n-type material is complicated by the inhomogeneity of samples. Current limitations to p-doping does not limit electronic and optoelectronic applications of ZnO, which usually require junctions of n-type and p-type material. Known p-type dopants include group-I elements Li, Na, K; group-V elements N, P and As; as well as copper and silver. However, many of these form deep acceptors and do not produce significant p-type conduction at room temperature. Electron mobility of ZnO strongly varies with temperature and has a maximum of ~2000 $cm^2/(V \cdot s)$ at 80 K. Data on hole mobility are scarce with values in the range 5–30 $cm^2/(V \cdot s)$.

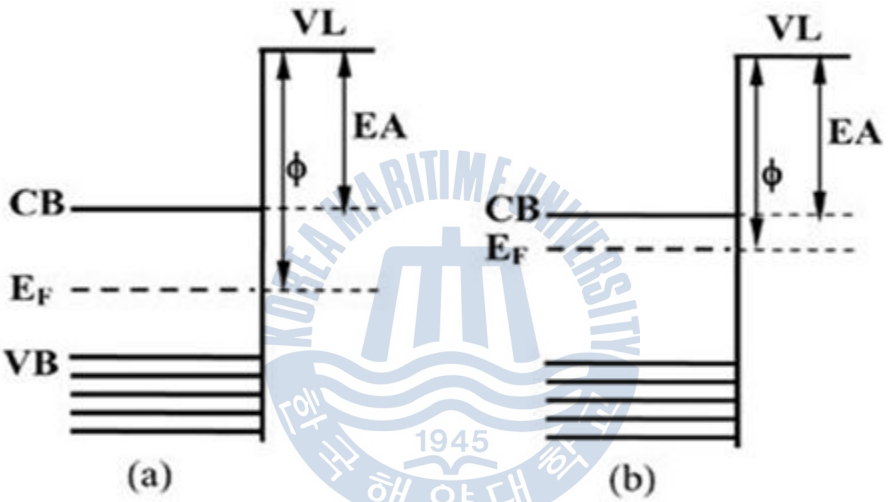

Fig. 3 Energy band level

(a) Energy level of ZnO

(b)Energy level of Group III element-doped ZnO

Table 1.. Electrical and physical properties of ZnO

Molecular mass	8.389
Specific gravity	5.642 g/cm^2
Point group	6 mm (wurtzite)
Lattice constant	a=3.249Åc=5.207Å
Mohs hardness	4
Dielectric constants	e_{11}=8.55, e_{33}=10.20□$^{-11}$ F/m
Thermal expansion coefficient	a_{11}=4.0, a_{33}=2.1(□$^{-6}$/℃)
Electron mass	0.28
Hole mass	1.8
Band gap energy at R.T	3.37 eV
Exviton binding energy	60 meV
Melting temperature	1975 ±25℃
Specific heat	0.125 cal
Thermal conductivity	0.006 cal/cmK

2.2 Transparent Conductive Oxide

Transparent conductive oxides (TCO) are doped metal oxides used in optoelectronic devices such as flat panel displays and photovoltaics (including inorganic devices, organic devices, and dye-sensitized solar cell). Most of these films are fabricated with polycrystalline or amorphous microstructures. On average, these applications use electrode materials that have greater than 80% transmittance of incident light as well as conductivities higher than 103 S/cm for efficient carrier transport. The transmittance of these films, just as in any transparent material, is limited by light scattering at defects and grain boundaries. In general, TCOs for use as thin-film electrodes in solar cells should have a minimum carrier concentration on the order of 10^{20} cm^{-3} for low resistivity and a bandgap lower than 380 nm to avoid absorption of light over most of the solar spectra. Mobility in these films is limited by ionized impurity scattering and is on the order of 40 $cm^2/(V \cdot s)$. Current transparent conducting oxides used in industry are primarily n-type conductors, meaning their primary conduction is as donors of electrons. Suitable p-type transparent conducting oxides are still being researched. To date, the industry standard in TCO is ITO, or tin-doped indium-oxide. This material boasts a low resistivity of ~10^{-4} Ω·cm and a

transmittance of greater than 80%. However ITO has the drawback of being expensive. Indium, the film's primary metal, is rare (6000 metric tons worldwide in 2006), and its price fluctuates due to market demand. For this reason, doped binary compounds such as aluminum-doped zinc-oxide (AZO) and indium-doped cadmium-oxide have been proposed as alternative materials. AZO is composed of aluminum and zinc, two common and inexpensive materials, while indium-doped cadmium oxide only uses indium in low concentrations. Binary compounds of metal oxides without any intentional impurity doping have also been developed for use as TCOs. These systems are typically n-type with a carrier concentration on the order of 10^{20} cm^{-3}, provided by interstitial metal ions and oxygen vacancies which both act as donors. However, these simple TCOs have not found practical use due to the high dependence of their electrical properties on temperature and oxygen partial pressure.

Table 2. Typical Transparent Conductive Materials

Type	Film Materials
Metal Film	Au, Ag, Pt, Cu, Rh, Pd, Al, Cr
Oxide-semiconductor film	In_2O_3, SnO_2, ZnO, CdO, TiO2, $CdIn_2O_4$, Cd_2SnO_2, Zn_2SnO_4, In_2O_3, ZnO, In_2O_3, SnO_2
Compound of Spinel-type	$MgInO_4$, $CaGaO_4$,
Conductive nitride film	TiN, ZrN, HfN
Compound of Conductive Boron	LaB_6
Etc.	Conductive Macromolecule

2.2.1 Theory

Charge carriers in these oxides arise from three fundamental sources: interstitial metal ion impurities, oxygen vacancies, and doping ions. The first two sources always act as electron donors; indeed, some TCOs are fabricated solely using these two intrinsic sources as carrier generators. When an oxygen vacancy is present in the lattice it acts as a doubly charged electron donor. In ITO, for example, each oxygen vacancy causes the neighboring In3+ ion 5s orbitals to be stabilized from the 5s conduction band by the missing bonds to the oxygen ion, while two electrons are trapped at the site due to charge neutrality effects. This stabilization of the 5s orbitals causes a formation of a donor level for the oxygen ion, determined to be 0.03 eV below the conduction band. Thus these defects act as shallow donors to the bulk crystal. Common notation for this doping is Kröger–Vink notation and is written as (2-1).

$$O_O^x \leftrightarrow V_O^{\bullet\bullet} + 0.5O_2(g) + 2e'$$

(2-1)

Here “O” in the subscripts indicates that both the initially bonded

oxygen and the vacancy that is produced lie on an oxygen lattice site, while the superscripts on the oxygen and vacancy indicate charge. Thus to enhance their electrical properties, ITO films and other transparent conducting oxides are grown in reducing environments, which encourage oxygen vacancy formation. Dopant ionization within the oxide occurs in the same way as in other semiconductor crystals. Shallow donors near the conduction band (n-type) allow electrons to be thermally excited into the conduction band, while acceptors near the valence band (p-type) allow electrons to jump from the valence band to the acceptor level, populating the valence band with holes. It is important to note that carrier scattering in these oxides arises primarily from ionized impurity scattering. Charged impurity ions and point defects have scattering cross-sections that are much greater than their neutral counterparts. Increasing the scattering decreases the mean-free path of the carriers in the oxide, which leads to poor device performance and a high resistivity. These materials can be modeled reasonably well by the free electron gas theory assuming a parabolic conduction band and doping levels above the Mott Criterion. This criterion states that an insulator such as an oxide can experience a composition-induced transition to a metallic state given a minimum doping concentration n_c, determined by (2-2).

$$n_c^{1/3} a_H^* = 0.26 \pm 0.05 \quad (2\text{-}2)$$

where a_H* is the mean ground state Bohr radius. For ITO, this value requires a minimum doping concentration of roughly 10^{19} cm^{-3}. Above this level, the typically electrically insulating material becomes metallic and is capable of allowing carrier flow.

2.2.2 Electrical properties of transparent conductive films

In cases where In_2O_3, a seed crystal of ITO is single crystal completely satisfying stoichiometric ratio, , electrons don't exist in conduction band at absolute zero but valence band moves in a insulated manner because it is fully filled with electrons. In_2O_3 has a crystalline structure called cubic bixbyite which belongs to cubic system. Among unit lattice in 1.011nm of lattice parameters, 32 units of In^{3+} and 48 units of O^{2-} are present and electrically neutral. In ion is six coordination in cubical structure, and two oxygen defects (quasi-anion-site) are coordinated. There are 2 kinds of coordination methods of 22 oxygen defects, b-site and d-site, instead of isotropic method. Each lattice has 8 and 24 of b-site and d-site, respectively. Distance between In^{3+} and O^{2-} atoms is 0.218 Å for d-site and 0.213 Å, 0.219 Å, and 0.233 Å for b-site with same numbers. The oxygen defects occur due to nonstoichiometric composition caused by extremely small reduction that the crystal

structures don't collapse. Since the oxygen vacancy forms donor level which releases 2 electrons, In_2O_3 has about $10^{18}\sim10^{19}cm^{-3}$ of carrier density. If Sn is doped in In_2O_3, quadrivalent Sn is substitutionally solidified in In site of trivalent. Substituted Sn releases 1 carrier per an atom 1atom and then is able to obtain $10^{20}\sim10^{21}cm^{-3}$of carrier density stably. However, practically it is not entirely solidified substitutionally and exists as interstitial atoms within crystalline. Also, as it forms neutral and ionic acid activation center, it causes a decrease of carrier mobility. Therefore, acid activation devices that cause a decrease of carrier mobility in degeneracy semiconductors are generally considered to be as follows (1) ionized impurities acid activation (2)neutral impurities acid activation (3)lattice vibration induced acid activation (4) charge induced acid activation (5) grain boundaries induced acid activation. The acid activation devices possess different temperature dependency so that the factors that influence the most on acid activation can be estimated by performing low temperature measurement of Hall Effect. In case of ITO thin films, the mobility is almost independent on low temperature, we can conclude that (3) and (4) acid activation devices are not important. Regarding (5), we can also conclude that grain boundaries acid activation is not significant as carrier acid activation with following reasons.

①Mean free path of ITO thin films is calculated using free electron gas

model. In result, it is small value with more than 1 digit compared to crystalline diameter

②Due to observation with high resolution TEM, non-crystalline and gaps in crystalline class is confirmed to be not existed because crystalline class is completely attached to the level on atom layers.

③Depending upon the manufacturing methods, ITO thin film with difference crystalline diameters from 10 to 1000nm can be made. However, there is no correlation between crystalline diameter and mobility.

Therefore, the carrier mobility in ITO thin films is mainly determined by (1) ionized impurities acid activation (2) neutral impurities acid activation. Ionized impurities acid activation center is oxygen defects releasing carriers and substituted Sn atom. According to Dingle theory, as carrier density increases, acid activation increases and mobility increases. The mobility decrease is inversely proportional by 2/3 power of carrier density so that specific resistance decreases if mobility is determined by only ionized impurities acid activation devices.

However, neutral impurities acid activation center doesn't contribute to the increase of carrier density and cause a decrease of mobility because Sn atom that is not involved in carrier release, SnO_2 complex, and lattice defects complex of In_2O_3 lattice etc are considered. In order to achieve low specific resistance, neutral impurities acid activation is

required to be limited to the minimum value.

2.2.3 Optical properties of transparent conductive films

ITO absorbs and reflects light in ultraviolet ray ranges and in infrared ray ranges, respectively, and penetrate light only in visible ray ranges. The threshold value on the short wavelength of the visible ray penetration windows is restricted by the energy gap of substance and the threshold value on the long wavelength is limited by plasma frequency which is the function of carrier density. Visible ray ranges have 380～76nm of light wavelength and 1.6～3.3eV of energy. Substances that energy-gap is greater than 3.3eV don't absorb light because electron band transition doesn't occur due to visible ray investigation. Absorption of visible rays is not occurred for In_2O_3 because In_2O_3 is a wide gap semiconductor with 3.75eV of band-gap; but it is transparent. Carries formed by oxygen defects and doped Sn have a wide band-gap on the exterior because of occupying the floors of conduction band so that Burstein-Moss(BM) shift which the threshold value of wavelength where the light is absorbed, the short wavelength of the visible ray penetration windows, is observed. The long wavelength of the visible ray penetration windows, the threshold value of wavelength where the light is reflected, is determined by

plasma frequency. When carriers count as plasma, collective longitudinal vibration of the carriers is the plasma frequency. Plasma frequency w P is defined by the equation below.

$$w_p{}^2 = \frac{nq^2}{em} - \frac{1}{\tau^2} \qquad (2\text{-}3)$$

In this equation, n, q, e, m, and τ represent carrier density, carrier current, permitivity, effective mass of carrier, and relaxation time, respectively. As ITO thin films have many electrons and exist as carriers, plasma assisted wavelength λ P that is calculated with plasma frequency is described as below if entire carriers are considered as electrons.

$$\lambda_P = \frac{2\pi c}{\left(\frac{ne^2}{em^*} - \frac{1}{r^2}\right)^{\frac{1}{2}}} \qquad (2\text{-}4)$$

In this equation, c, e, and m* indicate light velocity, current of the electrons, and effective mass of electrons, respectively. Light greater than λ P wavelength is reflected. In ITO, plasma assisted wavelength λ P is present in near infrared ray ranges. Whereas it reflects infrared rays, it penetrates visible rays. The plasma reflection is utilized in the application of hear reflective glass. As carrier density, n, increases, λ P

values decrease thereby moving to the short wavelength side. When used in display as transparent electrodes, the maximum value of the carrier density is determined at this point because reflection of visible rays should not be present.

2.2.4 Fabrication methods of transparent conductive films

The methods to manufacture ITO thin films includes the physical manufacturing process using the physical phenomena of vacuums which are represented as sputtering and vapor deposition and the chemical manufacturing process using chemical reaction including the spray method and CVD. They are classified like Fig 2.4.

1) Sputtering

Sputtering deposition is a procedure to deposit sputtered substances on the substrates in the vacuum. This procedure is roughly described in fig. 5. The method is not a chemical or thermal reaction; it is a method to make evaporative shape by mechanical procedure (using momentum) and has an advantage to use as target materials of certain materials. In general, DC method is used but RF charge with AC method can be used

in case of non-conductive target materials. Moreover, as glow discharge occurs in the method by using the objective treatments before coating as both poles, elimination of oxides and impurities on the surface is possible by utilizing sputtering and the coated layers have good adhesiveness because of surface activation.

1. RF magnetron sputtering

Radio frequency magnetron sputtering, also called RF magnetron sputtering is a process that is used to make thin film, especially when using materials that are non-conductive. In this process, a thin film is grown on a substrate that is placed in a vacuum chamber. Powerful magnets are used to ionize the target material and encourage it to settle on the substrate in the form of a thin film.

The first step in the RF magnetron sputtering process is to place a substrate material in a vacuum chamber. The air is then removed, and the target material, the material that will comprise the thin film, is released into the chamber in the form of a gas. Particles of this material are ionized through the use of powerful magnets. Now in the form of plasma, the negatively charged target material lines up on the substrate to form a thin film. Thin films can range in thickness from a few to a few hundred atoms or molecules.

The magnets help speed up the growth of the thin film because magnetizing the atoms helps to increase the percentage of target material that becomes ionized. Ionized atoms are more likely to interact with the other particles involved in the thin film process and are, therefore, more likely to settle on the substrate. This increases the efficiency of the thin film process, allowing them to grow more quickly and at lower pressures.

The RF magnetron sputtering process is especially useful for making thin films out of materials that are non-conducting. These materials may have more difficulty forming into a thin film because they become positively charged without the use of magnetism. Atoms with a positive charge will slow down the sputtering process and can “poison” other particles of the target material, further slowing down the process.

2. DC magnetron sputtering

DC magnetron sputtering is one of several types of sputtering, which is a method of physical vapor deposition of thin films of one material onto another material. The most common sputter deposition methods in use in 2011 are ion beam sputtering, diode sputtering and DC magnetron sputtering. Sputtering has a wide variety of scientific and industrial uses, and is one of the fastest growing production processes

used in modern manufacturing.

Very simply, sputtering occurs in a vacuum chamber, where a substance is bombarded with ionized gas molecules that displace atoms from the substance. These atoms fly off and hit a target material, called a substrate, and bond to it at an atomic level, creating a very thin film. This sputter deposition is done at an atomic level, so the film and the substrate have a virtually unbreakable bond and the process produces a film that is uniform, extremely thin and cost effective.

Magnetrons are used in the sputtering process to help control the path of the displaced atoms that fly randomly around the vacuum chamber. The chamber is filled with a low-pressure gas, frequently argon, and several high-voltage magnetron cathodes are placed behind the coating material target. High voltage flows from the magnetrons across the gas and creates high-energy plasma that strikes the coating material target. The force generated by these plasma ion strikes causes atoms to eject from the coating material and bond with the substrate.

The atoms that are ejected in the sputtering process usually fly through the chamber in random patterns. Magnetrons produce high-energy magnetic fields that can be positioned and manipulated to collect and contain the generated plasma around the substrate. This forces the ejected atoms to travel predictable paths to the substrate. By controlling the path of the atoms, the film deposition rate and thickness can also be

predicted and controlled.

Using DC magnetron sputtering allows engineers and scientists to calculate times and processes needed to produce specific film qualities. This is called process control, and it allows this technology to be used by industry in mass manufacturing operations. For instance, sputtering is used to create coatings for optical lenses used in items such as binoculars, telescopes and infrared and night-vision equipment. The computer industry uses CDs and DVDs that were manufactured using spluttering processes, and the semiconductor industry uses sputtering to coat many types of chips and wafers.

Modern high-efficiency insulated windows use glass that was coated using sputtering, and many hardware, toy and decorative items are manufactured using this process. Other industries that use sputtering include the aerospace, defense and automotive industries, the medical, energy, lighting and glass industries, and many others. Despite its already broad use, industry continues to find new uses for DC magnetron sputtering.

2) Electron Beam Depositing Process

Electron beam depositing process is a process where metal is evaporated through heating and the steam is deposited on the surface of

the substrate. It is hard to be used as LCD display, which requires flatness of the surface, since it uses steam. However, it is used in some portion in display industry sice crystallization can be easily adjusted by heat and thin films deposition speed is faster than sputtering process. Following picture describes deposition concept of electron beam depositing process.

3) CVD Process

CVD (Chemical Vapor Depositing) is a deposition process using chemical reaction. Unlike depositing thin film using physically, it is normally used when deposition for temperature sensitive substrate is required. CVD is usually used in Si metal, epitaxial growth of nitride and oxide, insulation protective film deposition of SiO_2 and SiN_4. Following picture describes deposition concept of CVD process.

4) PLD process

Pulsed laser deposition (PLD) is a thin film deposition technique where a high-power pulsed laser beam is focused inside a vacuum chamber to strike a target of the material that is to be deposited. This material is vaporized from the target (in a plasma plume) which deposits it as a

thin film on a substrate. This process can occur in ultra high vacuum or in the presence of a background gas, such as oxygen which is commonly used when depositing oxides to fully oxygenate the deposited films. While the basic-setup is simple relative to many other deposition techniques, the physical phenomena of laser-target interaction and film growth are quite complex. When the laser pulse is absorbed by the target, energy is first converted to electronic excitation and then into thermal, chemical and mechanical energy resulting in evaporation, ablation, plasma formation and even exfoliation. The ejected species expand into the surrounding vacuum in the form of a plume containing many energetic species including atoms, molecules, electrons, ions, clusters, particulates and molten globules, before depositing on the typically hot substra

5) Sol-Gel Process

Sol-Gel process is one of the liquid phase processes for thin film deposition. Sol is a suspension state where colloid, inorganic matter uni-molecular and solid molecular are dispersed. With the reaction progress of Sol, solid molecules become macromolecule and become solid network structure. At this point, Sol loses its liquidity and becomes Gel state. Also, by heating these Gel ceramics form of thin

film is produced. Productivity is excellent by producing thin film with Sol-Gel process, but transparency and conductivity of produced thin film is destabilized.

6) Plastering

Plastering process is known as wet coating and it is used in antistatic field. Plastering process produces transparent conductive thin film by heating and coating semiconductor oxide compound particle on polymer film using acryl resin solvent. Electrical conduction of plastering process is largely affected by the deposition heating temperature. Plastering process is usually used at electronic product to prevent static electricity, but now it is being studied to produce thin film with high transparency and high electrical conductivity.

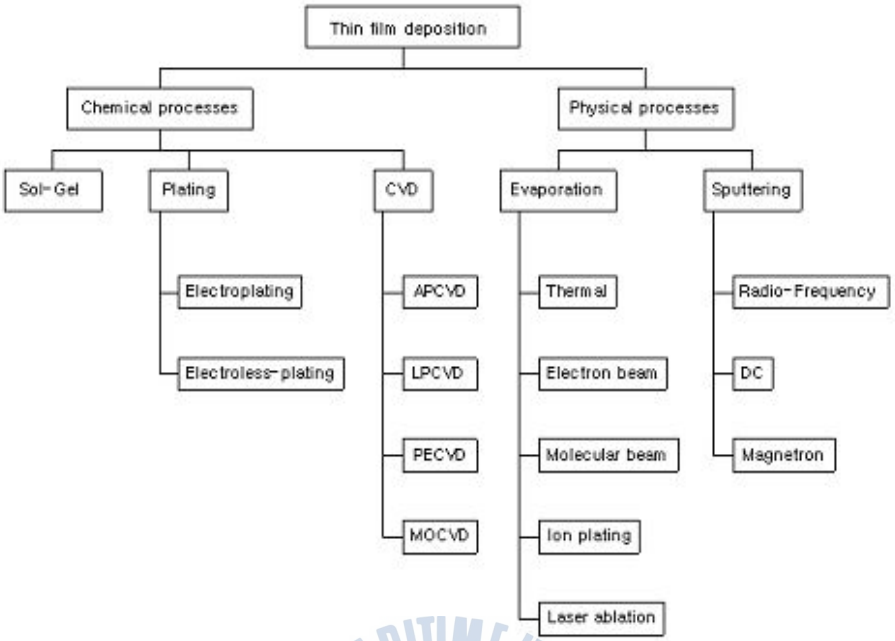

Fig. 4 Type of thin film depositon

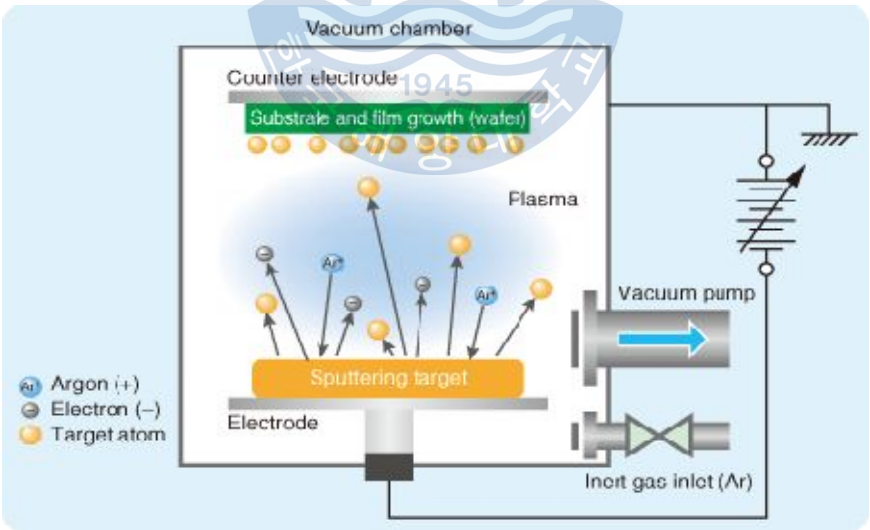

Fig. 5 RF magnetron sputtering system

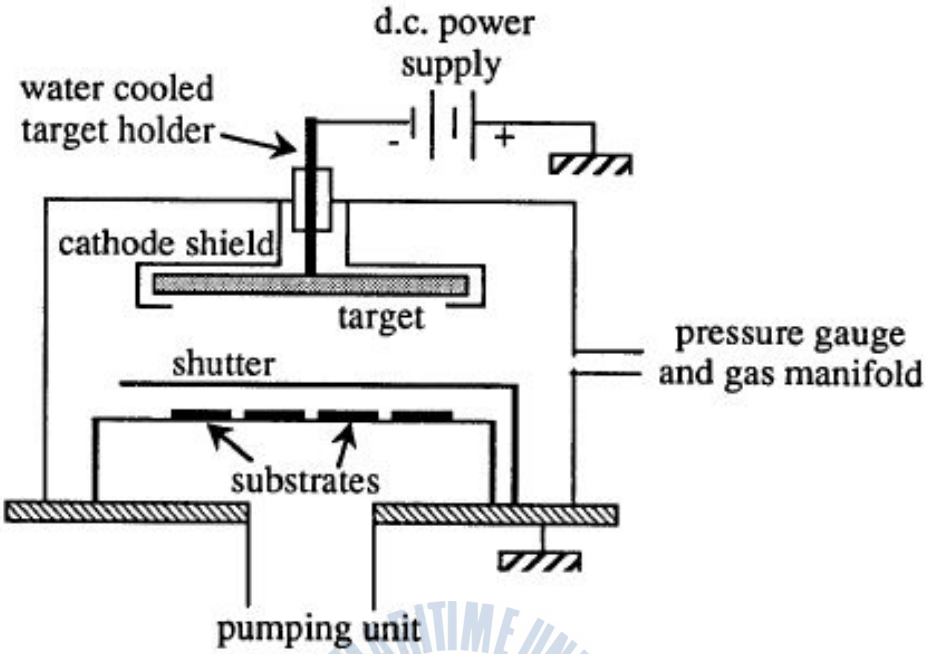

Fig. 6 DC magnetron sputtering system

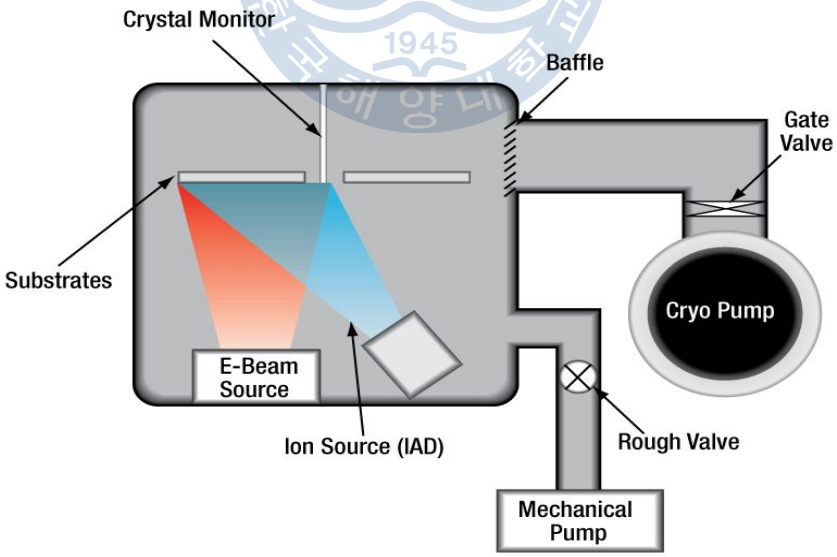

Fig. 7 Ion-Assisted E-Beam Deposition system

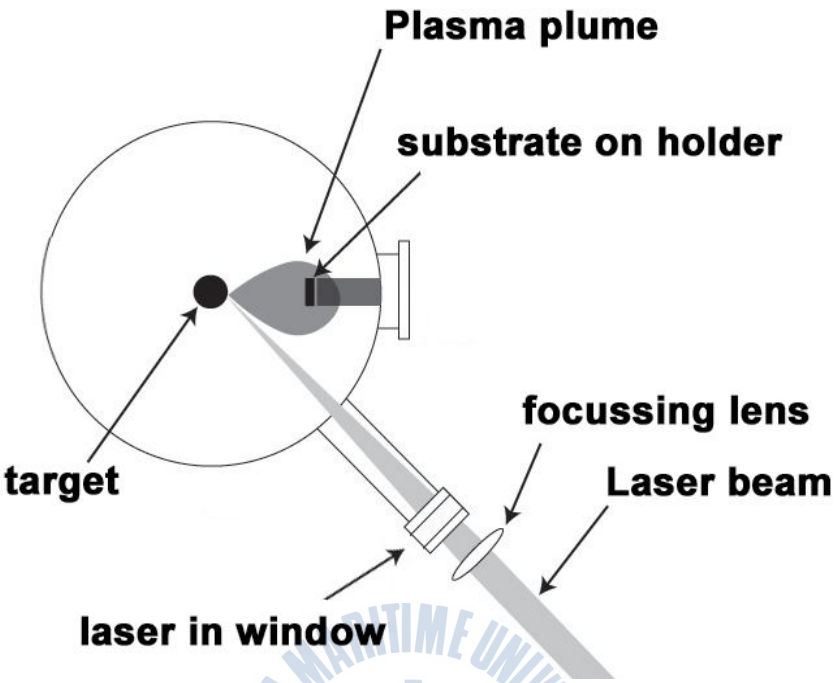

Fig. 8 Pulsed laser deposition process

2.4 Organic solar cell

An organic solar cell or plastic solar cell is a type of polymer solar cell that uses organic electronics, a branch of electronics that deals with conductive organic polymers or small organic molecules, for light absorption and charge transport to produce electricity from sunlight by the photovoltaic effect.

The plastic used in organic solar cells has low production costs in high volumes. Combined with the flexibility of organic molecules, organic solar cells are potentially cost-effective for photovoltaic applications. Molecular engineering can change the energy gap, which allows chemical change in these materials. The optical absorption coefficient of organic molecules is high, so a large amount of light can be absorbed with a small amount of materials. The main disadvantages associated with organic photovoltaic cells are low efficiency, low stability and low strength compared to inorganic photovoltaic cells.

The efficiency of the solar cell can be calculated the current-voltage curves PCE(Power Conversion Efficiency) defined by the following equation.

$$\mathrm{PCE} = \mathrm{FF} \times \frac{V_{OC} \times J_{SC}}{P_{input}} \tag{2.5}$$

$$FF = \frac{V_m \times I_m}{V_{oc} \times I_{sc}} \tag{2.6}$$

V_{oc} is open circuit voltage, J_{sc} is short circuit current density, FF is fill factor, P_{input} mean intensity of the incident light. V_m and I_m in fill factor represent the largest power. Maximum I_{sc} is 10mA/cm^2 in organic solar cell. This is compared to the silicon cell 1/3 levels. There is room improvement in changing optical and electrical properties. Overall this value stay 6% yet.

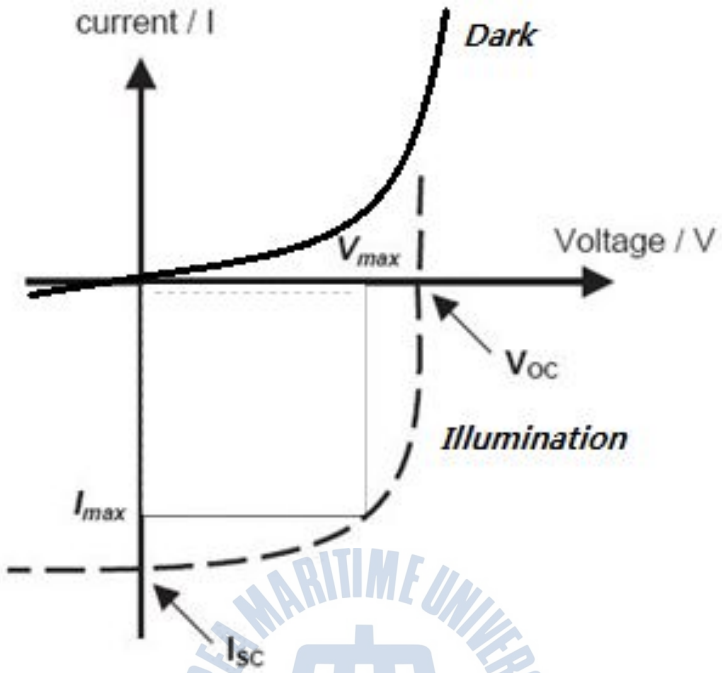

Fig. 9 The current-voltage curve of solar cell

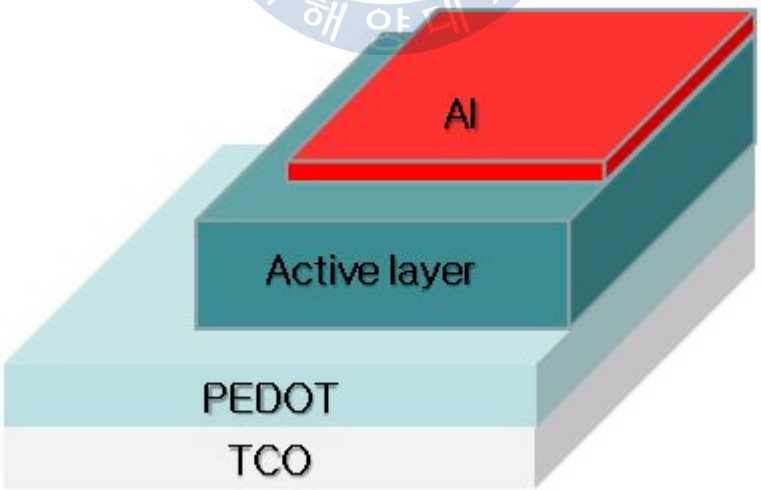

Fig. 10 General structure of organic solar cells

3. Experimental

3.1 Manufacture of AZO films

3.1.1 Equipment of Experimental

This study used the slope counter-target DC magnetron sputtering system as shown in Fig. 11. This system is the magnetron sputtering method that membrane is possible by the high speed in the atmosphere of low gas pressure of the low temperature substrate as doping of electron is done by action of the electric field and transverse magnetic field by applying the parallel magnetic field on the target surface and focusing plasma of the high density around the target.

The DC magnetron sputtering system used in this study has the characteristics that multi element films can be evaporated by the high speed by arranging the plural slope counter-target. When compared to the previous sputtering process, films of several types can be evaporated by easy control and the applicable scope is larger. The basic specifications of the system are as follow.

The slope counter-target DC magnetron sputtering system can evaporate sputtered particles efficiently because four counter targets are attached with angles. The mimetic diagram in the chamber of the device in this study is shown in Fig. 12.

Table 3. The specifications of the system

Method	Unstable equilibrium magnetron sputtering
Purpose	Deposition of multiple elements thin film
Composition	Separate form of main body and control unit
Pressure condition	Exhaustion time of gas: within 5 min to 2.6×10^{-3}Pa
Control method	DC power control, vacuum control system, heater control, gas flow control, control system of valve switch, manual control by panel computer
Electricity	200V 50/60Hz 3P, wring capacity: 100A
Cooling water	Above 0.1MPa and 14L/min, below 25℃ (in operation)
Air pressure	0.3 ~ 0.5 MPa
Gas	Ar 0.3 Mpa, high-purity(99.999%) O_2 0.3 Mpa, high-purity(99.999%)
Target	Zn (99.999%) : 300×48×t5 mm^3 Al (99.999%) : 300×48×t5 mm^3

Fig. 11 The inclination opposite target type DC magnetron sputtering equipment

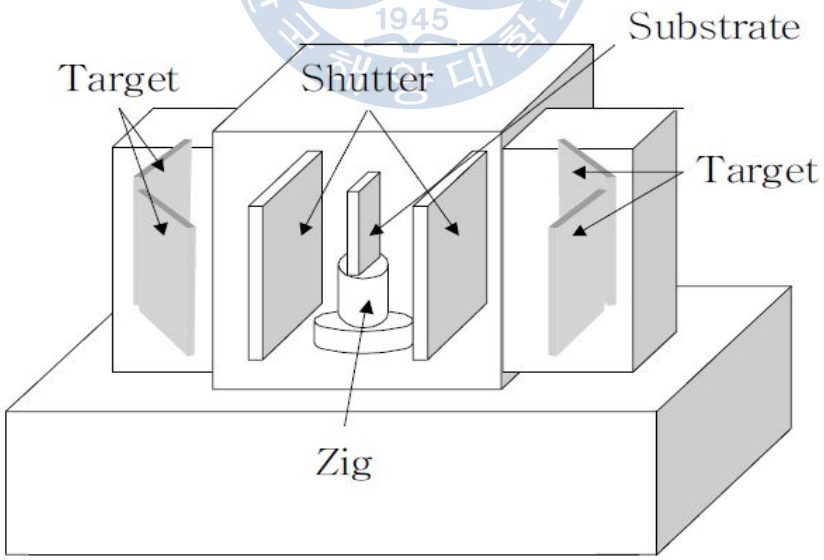

Fig. 12 Schematic diagram of inclination opposite target type DC magnetron sputtering equipment

3.1.2 Materials of experimental

Resistivity of transparent conductive used in display must be lower or same with metal wire, there need to be a new approach on structure or material. Therefore, in order to fulfill these purposes, transparent conductive multilayer thin film is getting its attention. Transparent conductive multilayer thin film deposits thin metal thin film layer between semiconductor oxide compound thin film layer like ITO and ZnO. Due to the metal thin film deposited in transparent conductive multilayer thin film, it produces excellent electrical conductivity and high permeability at visible range. In addition, it is possible to produce thin film with excellent durability than single layer metal thin film and thin film thickness thinner than semiconductor oxide compound thin film.

Aluminum is widely used in aerospace, transportation, construction field since it is light and against oxidation. Aluminum is also a good conductor and resistivity is 1.6 times copper. In room temperature, electrical conductivity and thermal conductivity (4~5 times of steel) is excellent. Therefore, aluminum has been made as thin film and used as element connector during semiconductor manufacturing process or optical element such as wave guidance and reflector. Following table shows metal's basic properties.

The experiment materials have been used to produce transparent conductive multilayer thin films by DC magnetron sputtering equipment in this study.

•Substrate: Slide glasses (L: 76mm, W: 26mm, T: 0.9 ~ 1.2)

Table 4. Fundamental properties of metals for thin film materials

	Zn	Al
Elementary name	Zinc	Aluminum
Elementary number	30	13
Atomic mass (g/mol)	65.38	26.9815396
Condition	Solid	Solid
Density (g/cm3)	7.14	2.70
Melting point (K)	692.68	933.47
Boiling point (K)	1180	2792
Magnetic characteristic	Diamagnetism	Paramagnetic
Electric resistance (Ωm)	59.0 X 10^{-6}	26.50 X 10^{-6}
Thermal conductivity	116 $Wm^{-1}K^{-1}$	237 $Wm^{-1}K^{-1}$
Thermal expansion coefficient	25 ℃	23.1 ℃

3.1.3 Experimental procedure

To manufacture transparent Conductive multilayer thin film, experiment was conducted by the following procedure.

1) Process before Experiment

1. Use Acetone and ethanol to conduct ultrasonic cleaning for 15 minutes and remove moisture on the surface using heat dryer.
2. Remove impure substanct inside the chamber of sputtering device.
3. Install target metal inside the chamber, and install specimen at the center.

2) Deposition of Thin Film

1. Install specimen and target metal, operate sputtering device to make the environment vacuum.
2. Inject reaction gas for 2 minute at the target metal and process sputtering for 5 minutes while the shutter of the chamber is closed. (Removing impure substance on the surface of target metal)
3. After removing impure substance on the surface of target metal, open the shutter and deposit thin film on the surface of the substrate. (ZnO: 4 hours, metal thin film: 30 min)
4. Calculate thickness of thin films which has completed deposition using Surface Profile Measuring System and divide it by

deposition time to calculate deposition rate of ZnO and Metal thin film.

5. Using the deposition rate, deposit ZnO and Metal thin film on glass substrate.
6. In order to produce transparent conductive multilayer thin film, deposit ZnO thin film and stop sputtering device and then deposit Metal thin film. Then deposit ZnO thin film once again on deposited Metal thin film to complete the structure of multilayer thin film. ※ Operate preliminary sputtering for 5 minute before depositing ZnO and Metal thin film while the chamber shutter is closed. (Removing impure substance on the surface of target metal)
7. Store substrate, which deposition of transparent conductive multilayer thin film complete, by each types of metal and deposition condition.

Following table shows deposition environment inside the chamber when thin film is deposited. Also, following diagram shows the image of Surface Profile Measuring System.

Table. 5 Sputtering condition of multilayer thin film.

Deposition parameters	**Conditions**
Base and working pressure	3 X 10^{-3} Pa, 6 ~ 7 X 10^{-1} Pa
Ar and O_2 partial pressure	50 sccm and 2 sccm
Working time and film thickness	4 Hours, 300 ~ 500 nm
Distance from target to substrate	30 cm
Zig rotation speed	12 rpm
Working temperature	Room temperature
Input power	
- ZnO cathode	DC magnetron mode
- Current	0.2 A
- Al cathode	DC magnetron mode
- Current:	1 ~ 8 mA

3.2 Measurement of the thin film thickness

The thickness of thin films is the very important factor to determine the properties of transparent conductive oxide films. The methods to measure the thin film thickness include Elipsometer, Stylus, Crystal Oscilators, VAMFO, CARIS, GravimetricTechnique, SEM, TEM, Color Chart, and RBS. SEM, TEM, and RBS of them are the measurement methods to investigate other characteristics rather than the thickness and the Color Chart is the subsidiary method to guess the rough thickness of transparent thin films.

Stylus means the method to measure height of step directly as the stylus which moves along the surface after forming step in thin films as one of the typical method to measure the thickness. The diamond needle stylus of radius 10 ㎛ is used. It can be measured within the scope of 200 Å ~65 ㎛. And resolution is about 10 Å. It has the disadvantage that it is difficult to measure the materials that it is difficult to form step, that is etching is difficult. This experiment measured it using Sloan DEKTAK 3030.

3.3 Optical property measurement

Ultravioletvisible spectroscopy or ultraviolet-visible spectrophotometry refers to absorption spectroscopy or reflectance spectroscopy in the ultraviolet-visible spectral region. This means it uses light in the visible and adjacent ranges. The absorption or reflectance in the visible range directly affects the perceived color of the chemicals involved. In this region of the electromagnetic spectrum, molecules undergo electronic transitions. This technique is complementary to fluorescence spectroscopy, in that fluorescence deals with transitions from the excited state to the ground state, while absorption measures transitions from the ground state to the excited state. Molecules containing π-electrons or non-bonding electrons can absorb the energy in the form of ultraviolet or visible light to excite these electrons to higher anti-bonding molecular orbitals. The more easily excited the electrons, the longer the wavelength of light it can absorb.

The instrument used in ultraviolet-visible spectroscopy is called a UV/Vis spectrophotometer. It measures the intensity of light passing through a sample (I), and compares it to the intensity of light before it passes through the sample (I_o). The ratio I/I_o is called the transmittance, and is usually expressed as a percentage (%T). The absorbance, A, is based on the transmittance.

$$A = -\log\left(\%\frac{T}{100}\%\right) \tag{3-1}$$

The UV-visible spectrophotometer can also be configured to measure reflectance. In this case, the spectrophotometer measures the intensity of light reflected from a sample (I), and compares it to the intensity of

light reflected from a reference material (I_o). The ratio I/I_o is called the reflectance, and is usually expressed as a percentage (%R).

In this research, UV-VIS-NIR spectrometer is used in order to measure permeability of transparent conductive AZO thin film. Spectrometer can irradiate certain light wavelength to sample by monochromator using prism or diffraction grating. At this point, permeability can be measured by comparing the amount of light first irradiated on the sample and amount of light passed the sample. UV-VIS-NIR spectrometer, used in this research, is a device which can irradiate three different kinds of light wavelength, including ultraviolet, visible spectrum ray, near infrared ray on the sample. In this study, however, in order to observe the optical characteristic of transparent conductive AZO thin film of general light, in the area of 200nm ~ 800nm visible wavelength light was used to measure the permeability of thin film.

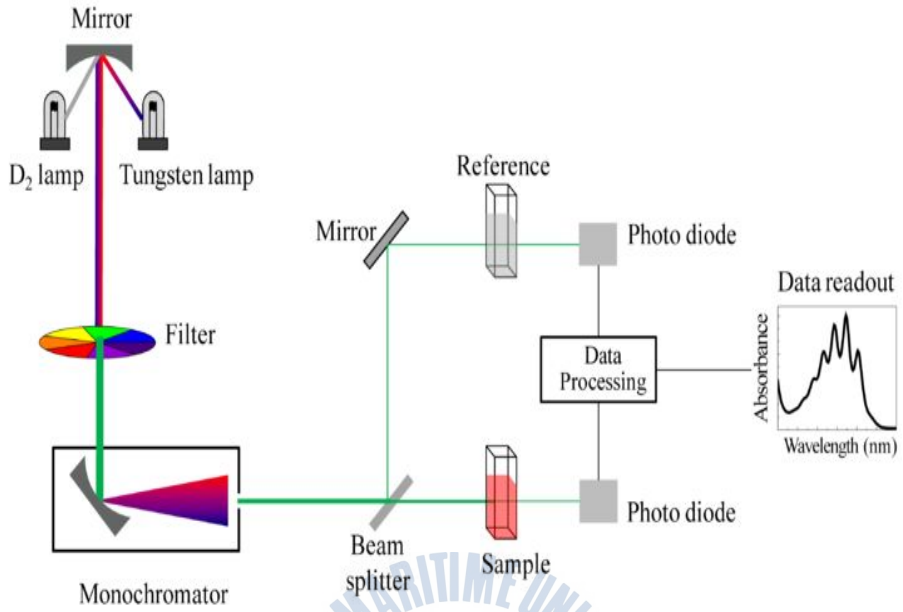

Fig. 13 Schematic diagram of UV- visible spectrophotometer

Fig. 14 The figure of UV-VIS-NIR spectrometer (V-570, Jasco)

3.4 The measurement of electric non-resistance of the thin film

The method to measure electric non-resistance includes two-point probe method, four-point probe method, and Van der Pauw method. But generally, four-point probe method is most used. Especially, the four-point probe method is very much used in the non-resistance measurement and surface resistance measurement because measurement is possible without any destroy of samples.

The basic properties of four-point probe method can reduce errors of the resistance value according to contact resistance, especially the measurement location by using the terminal for voltage which is separated from the current terminal. The measurement principle of the device is shown in Fig. 15

When a Kelvin connection is used, current is supplied via a pair of force connections. These generate a voltage drop across the impedance to be measured according to Ohm's law V=RI. This current also generates a voltage drop across the force wires themselves. To avoid including that in the measurement, a pair of sense connections are made immediately adjacent to the target impedance. The accuracy of the technique comes from the fact that almost no current flows in the sense wires, so the voltage drop V=RI is extremely low.

It is conventional to arrange the sense wires as the inside pair, while the force wires are the outside pair. If the force and sense connections are exchanged, accuracy can be affected, because more of the lead resistance is included in the measurement. In some arrangements, the force wires are very large, compared to the sense wires which can be

very small. If force and sense wires are exchanged at the instrument end, the sense wire could burn up from carrying the force current.

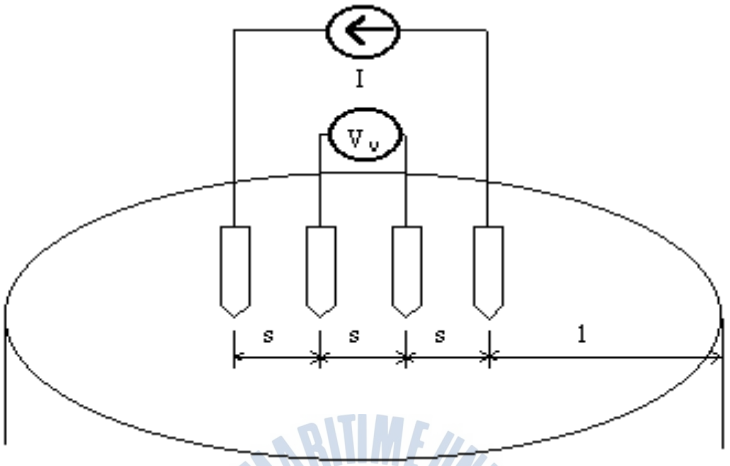

Fig. 15 Measurement of electrical resistivity by four-point probe method

3.5 Hall measurements

3.5.1 Background

When a charged particle—such as an electron—is placed in a magnetic field, it experiences a Lorentz force proportional to the strength of the field and the velocity at which it is traveling through it. This force is strongest when the direction of motion is perpendicular to the direction of the magnetic field; in this case the force

$$F_L = qvB \tag{3-2}$$

where q is the charge on the particle in coulombs, v the velocity it is traveling at (centimeters per second), and B the strength of the magnetic field (Wb/cm²). Note that centimeters are often used to measure length in the semiconductor industry, which is why they are used here instead of the SI units of meters.

When a current is applied to a piece of semiconducting material, this results in a steady flow of electrons through the material. The velocity the electrons are traveling at is (see electric current):

$$v = \frac{I}{nAq} \tag{3-3}$$

where is the electron density, is the cross-sectional area of the material and the elementary charge (1.602×10^{-19}coulombs).

If an external magnetic field is then applied perpendicular to the direction of current flow, then the resulting Lorentz force will cause the electrons to accumulate at one edge of the sample. Combining the above two equations, and noting that q is the charge on an electron, results in a formula for the Lorentz force experienced by the electrons:

$$F_L = \frac{IB}{nA} \tag{3-4}$$

This accumulation will create an electric field across the material due to the uneven distribution of charge, as shown in part (d) of the figure. This in turn leads to a potential difference across the material, known as the Hall voltage V_H. The current, however, continues to only flow along the material, which indicates that the force on the electrons due to the electric field balances the Lorentz force. Since the force on an

electron from an electric field □ is q, we can say that the strength of the electric field is therefore

$$\epsilon = \frac{IB}{qnA} \tag{3-5}$$

Finally, the magnitude of the Hall voltage is simply the strength of the electric field multiplied by the width of the material; that is,

$$\begin{aligned} V_H &= w\epsilon \\ &= \frac{wIB}{qnA} \\ &= \frac{IB}{qnd} \end{aligned} \tag{3-6}$$

where d is the depth of the material. Since the sheet density n_s is defined as the density of electrons multiplied by the depth of the material, we can define the Hall voltage in terms of the sheet density:

$$V_H = \frac{IB}{qn_s} \tag{3-7}$$

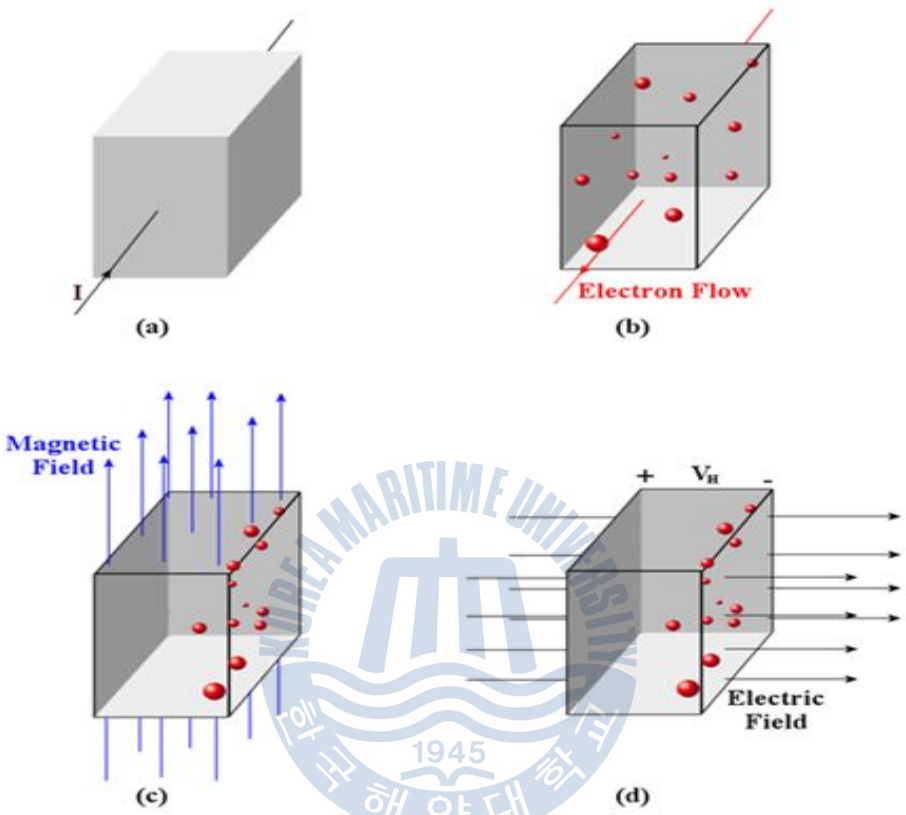

Fig. 16 The Hall effect as it is used for the van der Pauw method

(a) a current flowing through a piece of semiconductor material

(b) electrons flowing due to the current

(c) electrons accumulating at one edge due to the magnetic field

(d) resulting electric field and Hall voltage V_H

3.5.2 Making the measurements

Two sets of measurements need to be made: one with a magnetic field in the positive z-direction as shown above, and one with it in the negative z-direction. From here on in, the voltages recorded with a positive field will have a subscript P (for example, $V_{13,P}$) and those recorded with a negative field will have a subscript N (such as $V_{13,N}$). For all of the measurements, the magnitude of the injected current should be kept the same; the magnitude of the magnetic field needs to be the same in both directions also.

First of all with a positive magnetic field, the current I_{24} is applied to the sample and the voltage $V_{13,P}$ is recorded; note that the voltages can be positive or negative. This is then repeated for I_{13} and $V_{42,P}$.

As before, we can take advantage of the reciprocity theorem to provide a check on the accuracy of these measurements. If we reverse the direction of the currents (i.e. apply the current I_{42} and measure $V_{31,P}$, and repeat for I_{31} and $V_{24,P}$), then $V_{13,P}$ should be the same as $V_{31,P}$ to within a suitably small degree of error. Similarly, $V_{42,P}$ and $V_{24,P}$ should agree.

Having completed the measurements, a negative magnetic field is applied in place of the positive one, and the above procedure is repeated to obtain the voltage measurements $V_{13,N}$, $V_{42,N}$, $V_{31,N}$ and $V_{24,N}$.

3.4.2.3 Calculations

First of all, the difference of the voltages for positive and negative magnetic fields needs to be worked out:

$$V_{13} = V_{13,P} - V_{13,N}$$
$$V_{24} = V_{24,P} - V_{24,N}$$
$$V_{31} = V_{31,P} - V_{31,N} \quad (3\text{-}8)$$
$$V_{42} = V_{42,P} - V_{42,N}$$

The overall Hall voltage is then

$$V_H = \frac{V_{13} + V_{24} + V_{31} + V_{42}}{8} \quad (3\text{-}9)$$

The polarity of this Hall voltage indicates the type of material the sample is made of; if it is positive, the material is P-type, and if it is negative, the material is N-type.

The formula given in the background can then be rearranged to show that the sheet density

$$n_S = \frac{IB}{q|V_H|} \quad (3\text{-}10)$$

Note that the strength of the magnetic field B needs to be in units of Wb/cm². For instance, if the strength is given in the commonly used units of teslas, it can be converted by multiplying it by 10^{-4}.

3.4.2.4 Other calculations - Mobility

The resistivity of a semiconductor material can be shown to be

$$\rho = \frac{1}{q(n\mu_n + p\mu_p)} \quad (3\text{-}11)$$

where n and p are the concentration of electrons and holes in the material respectively, and μ_n and μ_p are the mobility of the electrons and holes respectively.

Generally, the material is sufficiently doped so that there is many orders-of-magnitude difference between the two concentrations, and so this equation can be simplified to

$$\rho = \frac{1}{q n_m \mu_m} \tag{3-12}$$

where n_m and μ_m are the doping level and mobility of the majority carrier respectively.

If we then note that the sheet resistance R_S is the resistivity divided by the thickness of the sample, and that the sheet density n_S is the doping level multiplied by the thickness, we can divide the equation through by the thickness to get

$$R_S = \frac{1}{q n_s \mu_m} \tag{3-13}$$

This can then be rearranged to give the majority carrier mobility in terms of the previously calculated sheet resistance and sheet density:

$$\mu_m = \frac{1}{q n_s R_s} \tag{3-14}$$

4. Result and discussion

4.1 Check of the growth structure by SEM picture

Fig. 17 and Fig. 18 shows the surface SEM images of the AZO thin films deposited at various Al target input current on the glass and PET substrate. The grain size increases with Al target input current. This is increased in 1mA by 8mA, conflicted Al-ions are increased. So, the number of ions increases coming from the target and particles increases the chance to reach the substrate. In addition, the al does the detergent role and the free energy required for the growth is lowered and the growth is promoted. It looks at to show altogether the same characteristic with glass and PET substrate. The grain size and growth rate can be controlled with Al target input current.

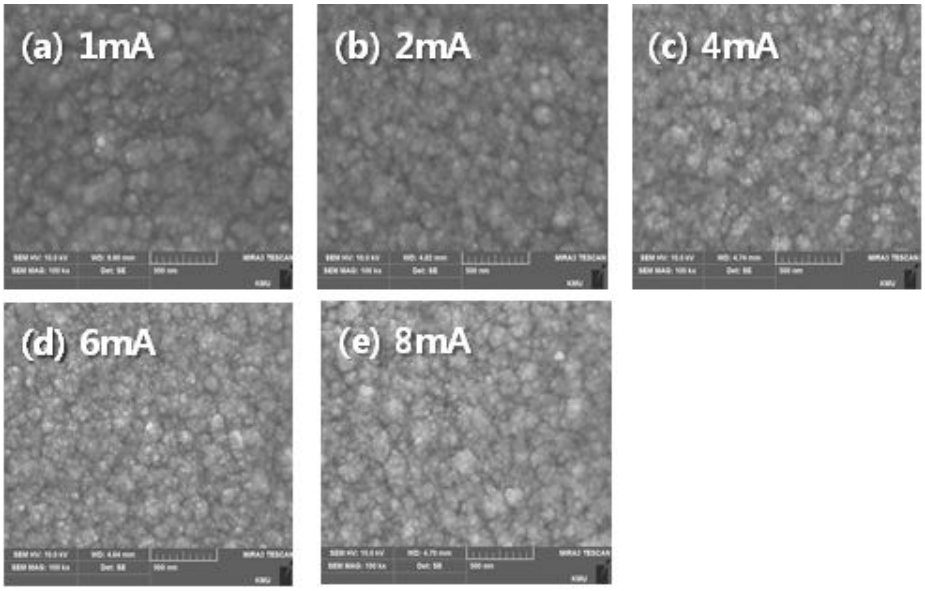

Fig. 17 Surface SEM images of the AZO thin films deposited at various Al target input current on the glass substrate.

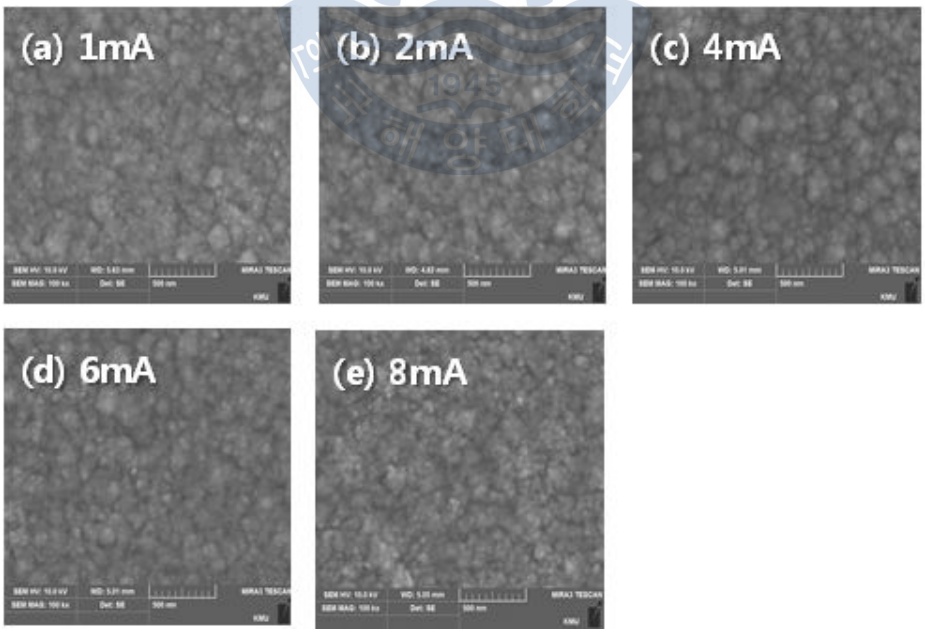

Fig. 18 Surface SEM images of the AZO thin films deposited at various Al target input current on the PET substrate.

4.2 Characteristics of optical transmittances as various Al target input current

To investigate characteristics of AZO thin films based on Glass substrate and PET substrate, optical and electric characteristics were compared by Al target input current. ZnO target input current is fixed, and Al target input current are varied 1, 2, 4, 6, 8 mA. The sample was deposited to a thickness of 300~500nm. Table 4.1 shows deposition condition.

Fig. 19 and Fig. 20 showed the transmittance spectra of AZO thin films deposited at various Al target input current. The graphs that the optical characteristics based on Al target input current. The graphs represented similar transmittance, indicating that there were no notable changes observed in optical characteristics since the deposition was carried out under the same conditions during the deposition of AZO thin films. 2mA and 4mA target input currents are demonstrate about 80% transmittance in the range of the visible spectrum, but the films deposited on 1mA, 6mA, 8mA demonstrate low transmittance. Given the changes in optical characteristics, it was observed that the target input current differences on the sputtering device affected on the formation of thin film structures. Therefore, it is highly recommended to perform deposition between 2mA and 4mA of target input current.

Table. 6 Sputtering condition of AZO thin films on Glass and PET substrate

Deposition parameters	**Conditions**
Base and working pressure	3 X 10^{-3} Pa, 6 ~ 7 X 10^{-1} Pa
Ar and O_2 partial pressure	50 sccm and 2 sccm
Working time and film thickness	4 Hours, 300 ~ 500 nm
Distance from target to substrate	30 cm
Zig rotation speed	12 rpm
Working temperature	Room temperature
Input power	
– ZnO cathode	DC magnetron mode
– Current	0.2 A
– Al cathode	DC magnetron mode
– Current:	1, 2, 4, 6, 8 mA

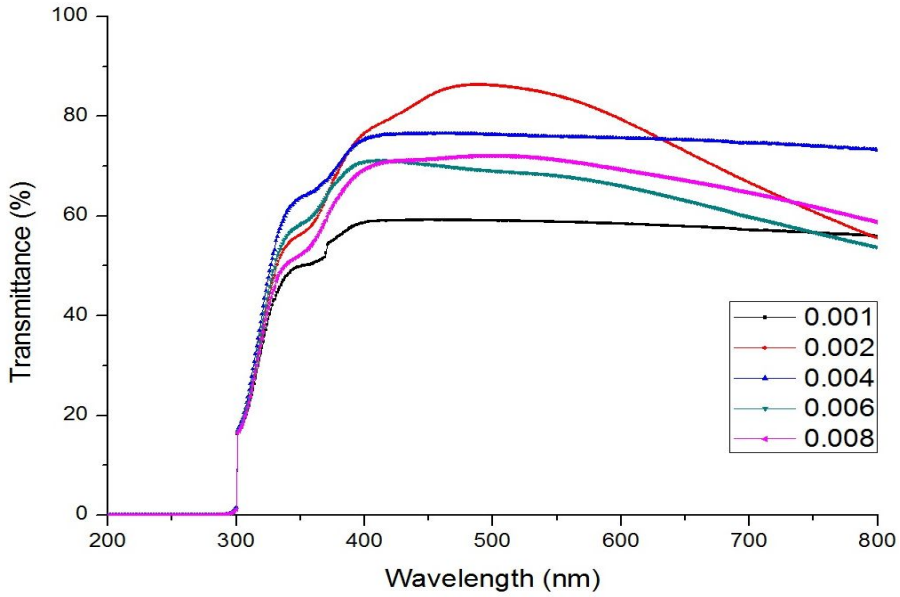

Fig. 19 Optical transmittances of AZO thin films prepared at Al target currents deposited on glass substrates

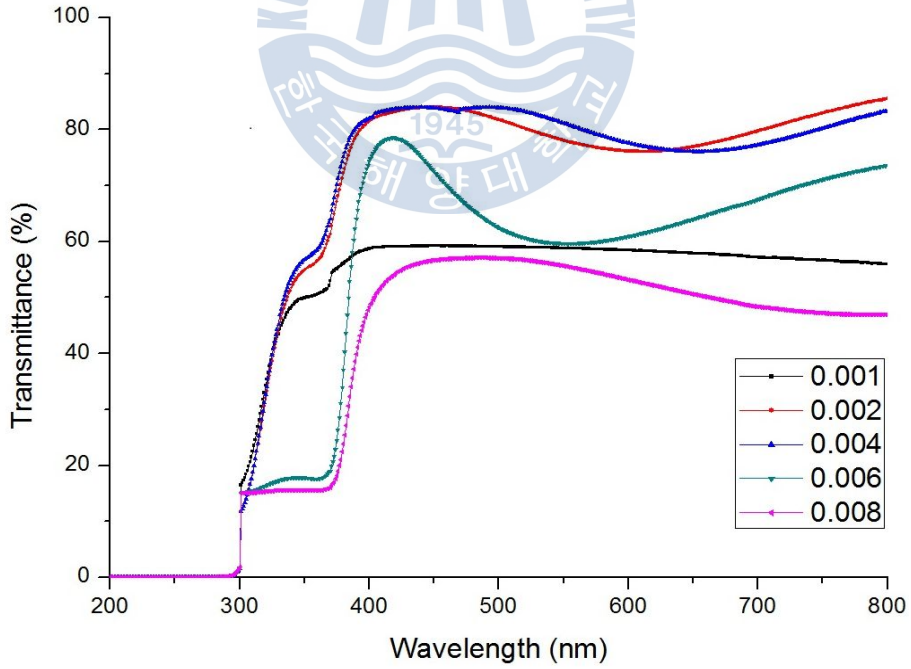

Fig. 20 Optical transmittances of AZO thinfilms prepared at Al target currents deposited on PET substrates

4.3 Electrical properties as various Al target input current

Fig. 21 and 22 shows the bulk concentration and mobility of AZO thin films deposited at various Al target input current. Graphs shows that when Al target input current is increase, the carrier concentration and mobility is increased. If Al target current increases, conflicted Al-ions are increased. Therefore the number of ions increases coming from the target and particles increases the chance to reach the substrate. As to this reason, the carrier by Al doping is due to be more than the carrier by the oxygen vacancy of the ZnO or the Zn interstitial element. Fig. 23 shows the sheet resistance of AZO thin films deposited at various Al currents from 1, 2, 4, 6, 8mA . When Al target input current was 6mA, sheet resistance is the smallest on glass and PET substrate. The minimum resistivity are 4.51×10^{-3}ohm/sq. and 3.96×10^{-3}ohm/sq. The sheet resistance reduced according to the increase in Al target input current. The sheet resistance is decreased because of the increase the concentration and mobility.

Fig. 24 and Fig. 25 show the electric properties of AZO thin films deposited at various Al currents from 1, 2, 4, 6, 8 mA. It's when the current of Al target when sputtering is done 6 mA in the experiment by raising the Al contents to find the most suitable Al contents of the AZO films. This case showed the best electrical characteristics.

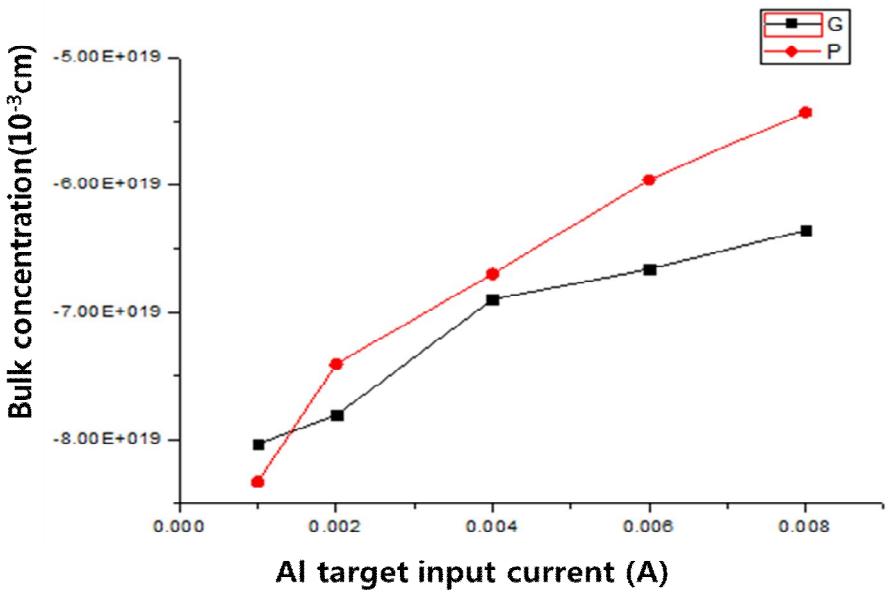

Fig. 21 Carrier concentration of AZO thinfilms prepared at Al target input current deposited on glass and PET substrates

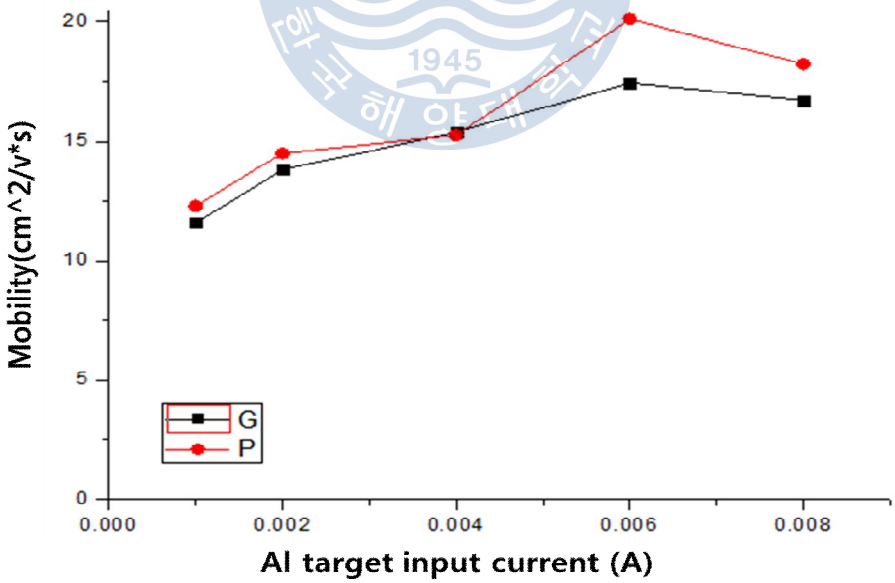

Fig. 22 Mobility of AZO thinfilms prepared at Al target input current deposited on glass and PET substrates

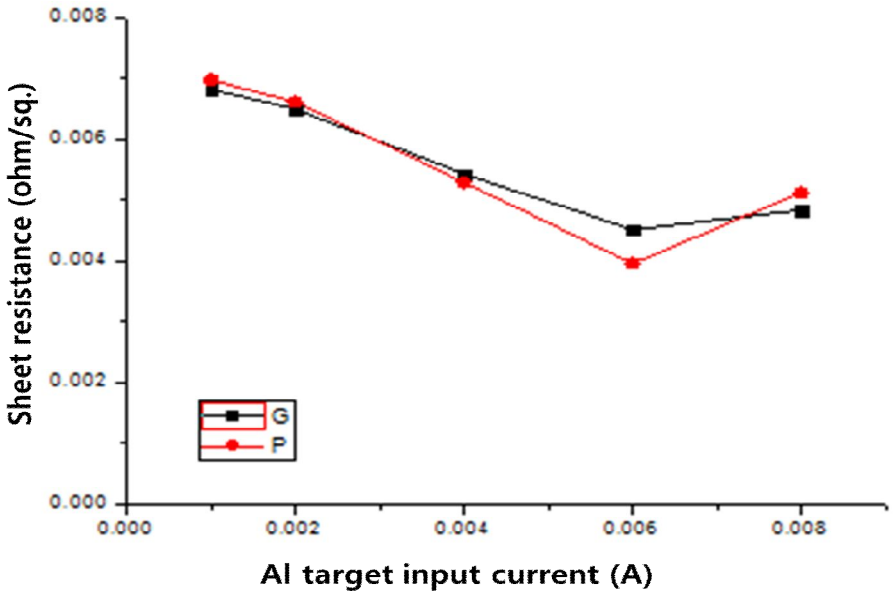

Fig. 23 Sheet resistance of AZO thin films prepared at Al target input current deposited on glass and PET substrates(G: galss substrate, P: PET substrate)

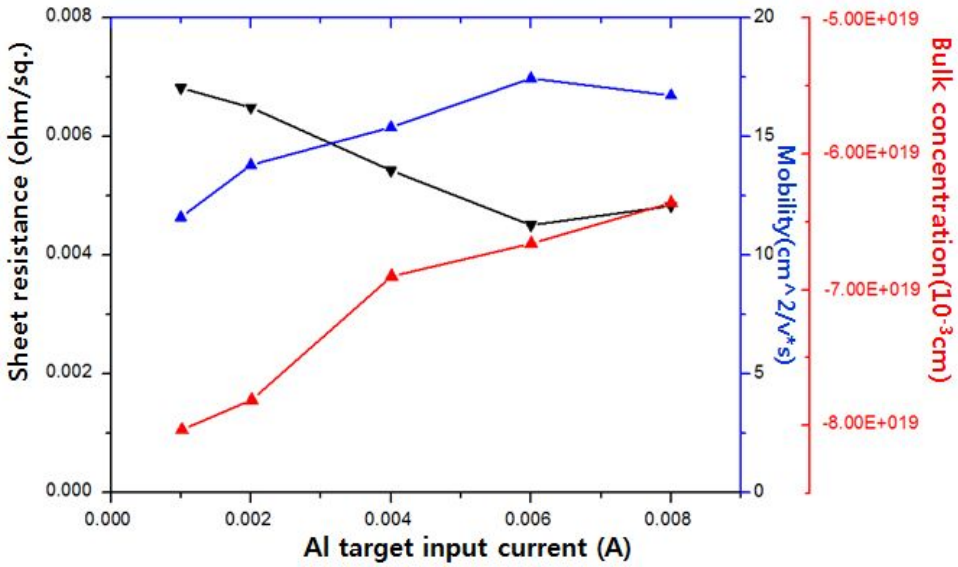

Fig. 24 Sheet resistance, carrier concentration, and mobility of AZO thinfilms prepared at Al target input current deposited on glass substrates

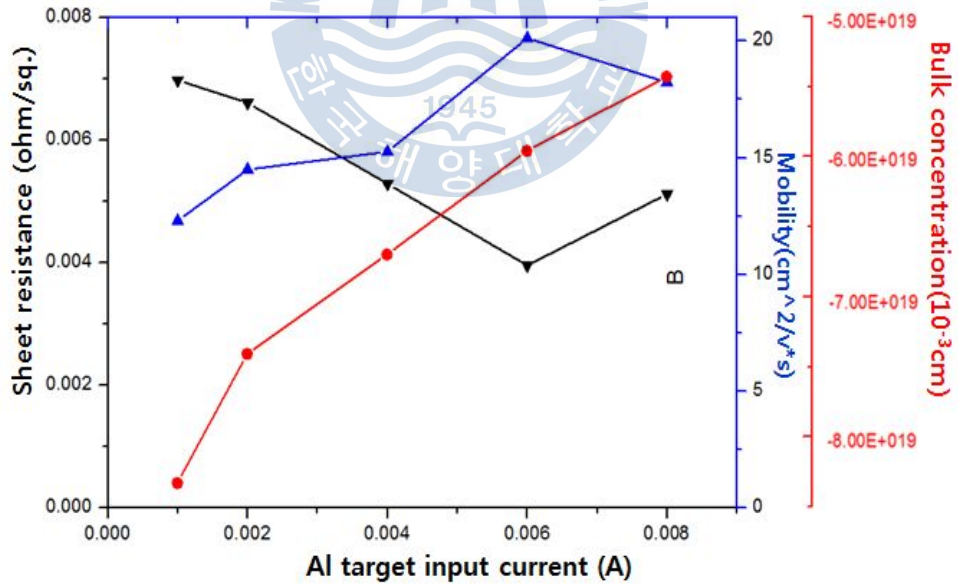

Fig. 25 Sheet resistance, carrier concentration, and mobility of AZO thinfilms prepared at Al target input current deposited on glass substrates

5. Conclusion

This paper is the study to check the growth of the micro structure when sputtering of Al doped ZnO is done at the different Al target input current and the effect of it on the optical and electrical properties. The input current of the Al target was measured in the DC magnetron sputtering system. Check of the growth of the micro structure was checked through the growth rate and SEM picture.

(1) The grain size increases with Al target input current. This is increased in 1mA by 8mA, the number of ions increases coming from the target and particles increases the chance to reach the substrate. In addition, the al does the detergent role and the free energy required for the growth is lowered and the growth is promoted. The grain size and growth rate can be controlled with Al target input current.

(2) When the Al target input current are 2mA and 4mA, it demonstrate about 80% transmittance in the range of the visible spectrum, but the films deposited on 1mA, 6mA, 8mA demonstrate low transmittance.

(3)If Al target input current increases in 1mA by 8mA, conflicted Al-ions are increased. So, the number of ions increases coming from the target and particles increases the chance to reach the substrate. Therefore the carrier by Al doping is due to be more than the carrier by the oxygen vacancy of the ZnO or the Zn interstitial element.

(4) When Al target input current was 6mA, sheet resistance is the smallest on glass and PET substrate. The minimum resistivity are 4.51×10^{-3}ohm/sq. and 3.96×10^{-3}ohm/sq. The sheet resistance is decreased because of the increase the concentration and mobility

(5) When the current of Al target when sputtering is done 6 mA in the experiment by raising the Al contents to find the most suitable Al contents of the AZO films.

The optical and electrical properties of the AZO films showed the result which is enought to use them for industry. Also, And given the changes in physical characteristics, it was observed that the target input current differences on the sputtering device affected on the formation of thin film structures.

Reference

[1] H.S. Ullal, K. Zwaibel, and B. Von Roedern, Proceedings of the 29th IEEE Photovolatic Specialists Conference, p. 472

[2] J. Pia, M. Tamasi, R. Rizzoli, M. Losurdo, E. Centurioni, C. Summonte, and F. Rubinelli, Thin Solid Films 425, 185 (2003)

[3] Y. H. Tak, K. B. Kim, H.G. Park, K.H. Lee, and J.R. Lee, Thin Solid Films 411, 12 (2002)

[4] H. Czternastek, Opto-Electronics Review 12, 49 (2004)

[5] Q. B. Ma, Z. Z. Ye, H. P. He, L. P. Zhu, J. R. Wnag, and B. H. Zhao, Materials letters 61, 2460 (2007)

[6] B. D. Ahn, S. H. Oh, C. H. Lee, G. H. Kim, H. J. Kim, and S. Y. Lee, J. Crystal Growth 309, 128 (2007)

[7] A. Teke, Ü. Özgür, S. Doan, X. Gu, H. Morkoç, B. Nemeth, J. Nause, and H. O. Everitt, Phys. Rev. B 70,195207(2004).

[8] B. K. Meyer, H. Alves, D. M. Hofmann, W. Kriegseis, D. Foster, F. Bertram, J. Christen, A. Hoffmann, M. Strassburg, M. Dworzak, U. Haboeck, and A. V. Rodina, Phys. Status Solidi B 241, 231 (2004).

[9] H. P. He, H. P. Tang, Z. Z. Ye, L. P. Zhu, B. H. Zhao, L. Wang, and X. H. Li, Appl. Phys. Lett. 90,023104(2007).

[10] Johannes Fallert, Robert Hauschild, Felix Stelzl, Alex Urban, Markus Wissinger, Huijuan Zhou, Claus Klingshirn, and Heinz Kalt, J. Appl. Phys. 101, 073506 (2007)

[11] H. M. Hiep et al. (2007). "A localized surface plasmon resonance based immunosensor for the detection of casein in milk" (free download pdf). Sci. Technol. Adv. Mater. 8 (4): 331. Bibcode 2007STAdM...8..331M. doi:10.1016/j.stam.2006.12.010.

[12] S. Pillai, K. R. Catchpole, T. Trupke and M. A. Green (2007).

"Surface plasmon enhanced silicon solar cells". J. Appl. Phys. 101 (9): 093105. Bibcode 2007JAP...101i3105P. doi:10.1063/1.2734885.

[13] C. Budesman et al, "Transparent conductive Zinc Oxide, Chapter3 (2007) 82 Springer.

[14] Richard A. Swalin "Thermodynamics of Solids", JOHN WILEY & SONS, pp 335. 341,(1972).

[15] N. Y. Lee, K. J. Lee, J. E. Kim, H. Y. Kwak, H. C. Lee, H. Lim, J. Appl. Phys. 78, 3367, (1995)

[16] Z.C. Jin, I. Hamberg, C.G. Granqvist, J. Appl. Phys. 64 (1988) 5117

[17] Thin Solid Films 293(1997) 117-123.

[18] B. E. Semelius, K. .F. Berggren, Z. .C. Jin, I. Hamberg and C. G. Granqvist, Phys. Rev.B, 37, 10244 (1988)

[19] He, Yue-Song, Campbell, Joe C., Murphy, Robert C., Arendt, M. F. and Swinnea, John S., Journal of Materials Research, 8 (1993) 3131.

[20] Lowry, M. S., Hubble, D. R., Wressell, A. L., Vratsanos, M. S., Pepe, F. R. and Hegedus, C. R., Journal of Coatings Technology Research, 5 (2008) 233.

[21] Van der Pauw, L.J. (1958). "A method of measuring specific resistivity and Hall effect of discs of arbitrary shape" (http:/ / astro1. panet.utoledo. edu/ ~relling2/ teach/ 6180-7180/ Hall_effect_van der Pauw_1958. pdf) (PDF). Philips Research Reports 13: 1–9.

[22] K. Vanheusden, W.L. Warren, C.H. Seager, D.R. Tallant, J.A. Voigt, B.E. Gnade, J. Appl. Phys. 79 (1996) 7983.

[23] K.L. Chopra, S. Major, D.K. Pandya, Thin Solid Films 102 (1983)

[24] K.H. Kim, T.S. Park, J. Kor. Phys. Soc. 18 (1985) 124.

[25] C.G. Granqvist, Thin Solid Films (1990) 730, pp.193-194

[26] B.S Kim, S.K Kim and Y.S Kim, submitted to Journal of the Korean Ceramic Society, Vol. 43, No. 9 (2006), pp. 532-536

[27] D.H Kim, R.I. Murakami and Y.H. Kim, Advanced Materials Research Vols. 97-101 (2010) pp 1768-1771

[28] S. k. Lee, S. J. Kwak, M. H. Lee, D. H. Seo, S. H. Shin, K. H. Choi, ” The Optical Technology of Polymeric Films for the Next Generation Display”, Polymer Science and Technology Vol. 19, No. 6, (2008)

[29] H. K. Pulker, Coating on Glass (Elsevier, Amsterdam, 1984), chap. 6.

[30] C. K. Hwangbo, Thin Film Deposition (Dasan Publisher, Seoul, 2001), PP. 152.

[31] M. Ohring, The materials science of thin films (Academic Press, San Diego, 1992), chap. 3

[32] N. Kaiser, and H. K. Pulker, ed., Optical Interference Coatings(Springer-Verlag Berlin Heidelberg New York, 2003), PP. 64-68

[33] D. E. Aspnes, "Optical properties of thin films," Thin Solid Films 89,249-262 (1982).

[34] K. H. Gienther, D. J. Smith, and L. Bangjun, "Structure and related properties of thin film optical coatings,: in Optical Thin Films II-. New Developments, R. T. Seddon, ed., Proc. SPIE 678, 2-11 (1986).

[35] H. A. Macleod, "Microstructure of optical thin films," in Optical Thin Films, R. T. Seddon, ed., Proc. SPIE 325, 21-29 (1982)

[36] S. Y. Choi, J. S. Kim, D. Y. Ma, W. D. Park, K. M. Choi, K. W. Kim, Basig of Thin Film Deposition (Iljin Corporation, Seoul, 2006), PP.106-110.

[37] G. Attard, and C. Barnes, Surfaces (Oxford University Press, New York,1998), PP 1-36.

[38] N. Kaiser, "Review of the fundamentals of thin-film growth," Appl. Opt.41(16), 3053-3060 (2002).

[39] B. A, Movchan and A. V. Demchishin, "Rosti struktura tonkich tverdotelnych plenok," Phys. Met. Metallogr. 28, 83-91

(1969).

[40] J. A. Thornton, "Influence of apparatus geometry and deposition conditions on the structure and topography of thick sputtered coatings," J. Vac. Sci. Technol. 11, 666-672 (1974).

[41] R. Messier, A. P. Giri, and R. A. Roy, "Reveised structure zone model for thin film physical structure," J. Vac, Sci. Technol. A 2, 500-503 (1984).

[42] A. G. Dirks, and H. J. Leamy, "Columnar microstructure in vapor-deposited thin film," Thin Solid Films 47, 219-233 (1997).